Structural Transition in Atomic Chains Driven by Transient Doping

S. Polei,[1] P. C. Snijders,[2] S. C. Erwin,[3] F. J. Himpsel,[4] K-H. Meiwes-Broer,[1] and I. Barke[1,*]

[1]*Department of Physics, University of Rostock, D-18051 Rostock, Germany*

[2]*Materials Science and Technology Division, Oak Ridge National Laboratory, Oak Ridge, Tennessee 37831, USA and Department of Physics and Astronomy, The University of Tennessee, Knoxville, Tennessee 37996, USA*

[3]*Center for Computational Materials Science, Naval Research Laboratory, Washington, DC 20375, USA*

[4]*Department of Physics, University of Wisconsin-Madison, Madison, Wisconsin 53706, USA*

(Received 30 April 2013; published 8 October 2013)

A reversible structural transition is observed on Si(553)-Au by scanning tunneling microscopy, triggered by electrons injected from the tip into the surface. The periodicity of atomic chains near the step edges changes from the 1×3 ground state to a 1×2 excited state with increasing tunneling current. The threshold current for this transition is reduced at lower temperatures. In conjunction with first-principles density-functional calculations it is shown that the 1×2 phase is created by temporary doping of the atom chains. Random telegraph fluctuations between two levels of the tunneling current provide direct access to the dynamics of the phase transition, revealing lifetimes in the millisecond range.

DOI: 10.1103/PhysRevLett.111.156801 PACS numbers: 73.20.−r, 61.72.U−, 68.35.Rh, 68.37.Ef

Transient, nonequilibrium electronic phases have generated excitement in both fundamental and applied physics by providing access to hidden states of matter not accessible by static measurements [1]. Prominent examples include the formation of excimers [2], photon-induced *cis-trans* isomers in molecular systems [3], highly excited clusters and nanoparticles [4,5], and structural dynamics in VO_2 [6]. Time-resolved methods such as pump-probe techniques provide access to such phenomena. Recently, it has become possible to resolve *cis-trans* isomers spatially and to switch individual molecules and molecular layers on metal surfaces (see Ref. [7] for a review).

To study changes in atomic configuration in real space, high-resolution microscopy such as scanning tunneling microscopy (STM) is necessary. The STM tip can serve as both excitation source and local probe. Tip-induced excitations of surface structures have been observed in several previous studies [8–13]. Various excitation mechanisms have been proposed, including strong electric fields [14], short-range forces [8,15], surface charging [16,17], and inelastic electron scattering [10]. Current-induced changes have been reported, such as flipping of asymmetric dimers [9,18,19] and of molecules [20,21], as well as switching of the local symmetry of a surface reconstruction [11,17]. These systems typically have two (meta)stable states separated an energy barrier. The tunneling electrons (or other excitation sources) provide the energy needed to overcome the barrier, allowing the system to switch between states [9,10].

Here we report the observation of a transient excitation in one-dimensional (1D) atomic chains on Si(553)-Au from the ground state to a nonequilibrium state. The Si(553)-Au system has been the topic of intense research due to its unique electronic and structural properties [22–31]. Previous studies addressed the static features of this surface. Here we inject electrons from the STM tip and find that the resulting electron doping causes a structural phase transition at sufficiently high currents. After a characteristic residence time this excited state collapses spontaneously by draining the excess charge into the bulk, allowing the system to relax back to its ground state. Density-functional theory (DFT) calculations of total energy versus electron doping indeed predict two phases with 1×3 and 1×2 periodicities, in accordance with the observations.

Our results enable the study of doping-dependent phase diagrams in 1D systems, despite the fact that doping of such systems is notoriously difficult due to the structural disorder created by the dopants and the associated electronic localization [32].

The experiments were performed in a commercial low-temperature STM system (Omicron Nanotechnology) operated between 7 and 63 K. The surface was prepared on Si(553) (0.01–0.03 Ω cm, *p*-type) following procedures in Ref. [33]. This results in a well defined Si(553)-Au reconstruction with low defect density (Fig. 1). Electrochemically etched Cr and W tips were used. Control experiments gave identical results for both tip materials. All data were recorded with tip-sample voltages between 1.0 and 1.3 V; no pronounced voltage dependence was observed.

For the DFT calculations the Si(553)-Au surface was represented by six layers of Si plus the reconstructed top surface layer with a 1×6 unit cell and a vacuum region of 10 Å. Total energies and forces were calculated within the generalized-gradient approximation of Perdew, Burke, and Ernzerhof using projector-augmented wave potentials, as implemented in VASP [34,35]. All atoms were free to move except the bottom Si layer and its passivating hydrogen layer. The plane-wave cutoff was 250 eV and the surface

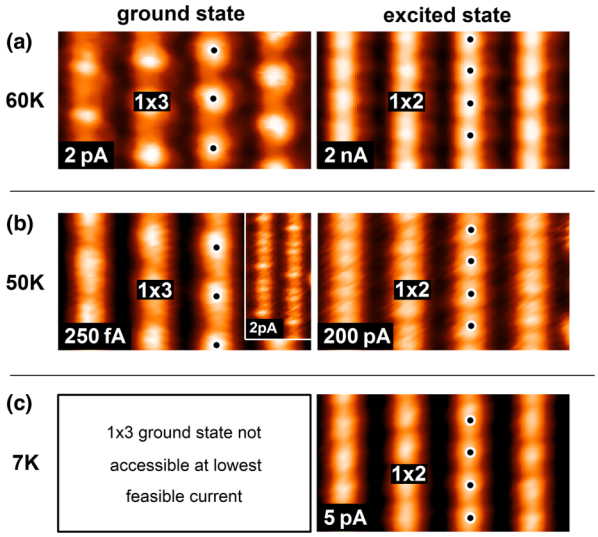

FIG. 1 (color online). STM topography [(6.0×3.3) nm^2] at different temperatures and current set points. For low currents a 1×3 structure is observed (left column). The periodicity changes to 1×2 at high currents (right column). With decreasing temperature the transition between the two structures occurs at progressively lower currents, falling below our experimental limit at 7 K (c). Near the transition current a mixture of the 1×2 and 1×3 structures is visible, resulting in an apparent 1×6 periodicity [inset to (b), (3.2×6) nm^2].

Brillouin zone was sampled using a 2×4 grid. The ground state of the neutral system has 1×3 periodicity along the Si step edge and exhibits a metastable 1×2 state with higher energy. The change in energy of these initial phases upon electron doping was determined by systematically varying the doping level and, at each level, fully relaxing the structure. The doping was done in two different ways with identical results: implicitly, by adding electrons to the system with a compensating uniform background charge; and explicitly, by substitutional doping on either the passivating hydrogen sites or on bulklike Si sites.

The left-hand side of Fig. 1(a) shows the STM topography of Si(553)-Au at 60 K and low current (2 pA). Bright protrusions with 1×3 periodicity are visible on the Si step edges, in agreement with earlier studies [26,28]. When imaged at the same temperature with higher current [2 nA; see the right-hand side of Fig. 1(a)], the surface undergoes a reorganization to a new periodicity of 1×2 which is slightly displaced by ≈ 1 Å towards the adjacent Au chain on the same terrace. These findings confirm previous observations of both periodicities near the Si step edges [26] but in addition suggest that the surface can be switched back and forth between these phases by varying the tunneling current. Figure 1 shows that this effect is not restricted to a particular location but is observed over extended areas. At intermediate currents a gradual transition of 1×3 to 1×2 is observed (see the movie in the Supplemental Material [36]) in which the topography can be described by a linear combination of the low and high current phase [37]. At slightly lower temperature the same transition occurs at lower currents [see Fig. 1(b)] while at 50 K a current considerably below 1 pA is needed to observe the 1×3 structure [see the left-hand side of Fig. 1(b)]. For example, at 2 pA a significant admixture of the 1×2 phase is present, resulting in an overall 1×6 appearance [see the inset in Fig. 1(b)] [38]. At much lower temperatures [see Fig. 1(c)], the 1×2 phase is triggered even by the lowest current available in our experiment. At a given temperature, the 1×2 phase is always observed at higher currents while the 1×3 phase is observed at lower current (if it is accessible). Hence the 1×2 phase represents an excited state of the the 1×3 ground state. The excitation probability increases with decreasing temperature. Rapid fluctuations occasionally found in STM images (see the Supplemental Material [36]) suggest that the surface structure quickly switches between the two states. STM images without apparent fluctuations correspond to a time average of the contributing states [see the inset of Fig. 1(b)].

The dynamics of the phase transition are revealed by time dependent changes in the current due to differences in the apparent topography. Figure 2(a) shows that the transient current, at constant tip-sample separation (i.e., feedback loop disabled) atop a bright protrusion of the 1×3 reconstruction, exhibits a random telegraph signal (RTS) on a time scale of milliseconds, confirming the dynamic nature of the phase transition. Figure 2(b) shows current histograms for different average tunneling currents. They consist of two distinct Gaussian peaks. Their horizontal separations represent the mean amplitude of current fluctuations while their widths arise from Gaussian noise in the current. A RTS is fully characterized by its amplitude and the average lifetimes (inverse excitation or decay rate) $\langle \tau_0 \rangle$ and $\langle \tau_1 \rangle$ of the ground and excited state, respectively. The ratio $\langle \tau_1 \rangle / \langle \tau_0 \rangle$ corresponds to the ratio of the areas A_0 and A_1 under the Gaussian peaks [see Fig. 2(b)]. Here we identified which transient current magnitude corresponds to the ground and excited state by noting that with increasing average tunneling current, the fraction of time the system resides in the excited state should increase. Peak A_1 therefore corresponds to the excited state, and peak A_0 to the ground state. This implies that the topographic change due to the transition to the 1×2 state (as measured above the bright protrusions of the 1×3 state) results in a decreased current; this explains why peak A_1 is to the left of peak A_0.

More detailed information on the underlying mechanism of the fluctuations can be obtained from the dependence of $\langle \tau_0 \rangle$ and $\langle \tau_1 \rangle$ on the current. Statistical analysis of the time traces, using a threshold method similar to the one in Ref. [39], and exponential fitting of the residence time distributions in ground and excited states [see Fig. 2(c)] for different currents, yields the dependence shown in Fig. 2(d). Interestingly, $\langle \tau_0 \rangle$ decreases as a function of

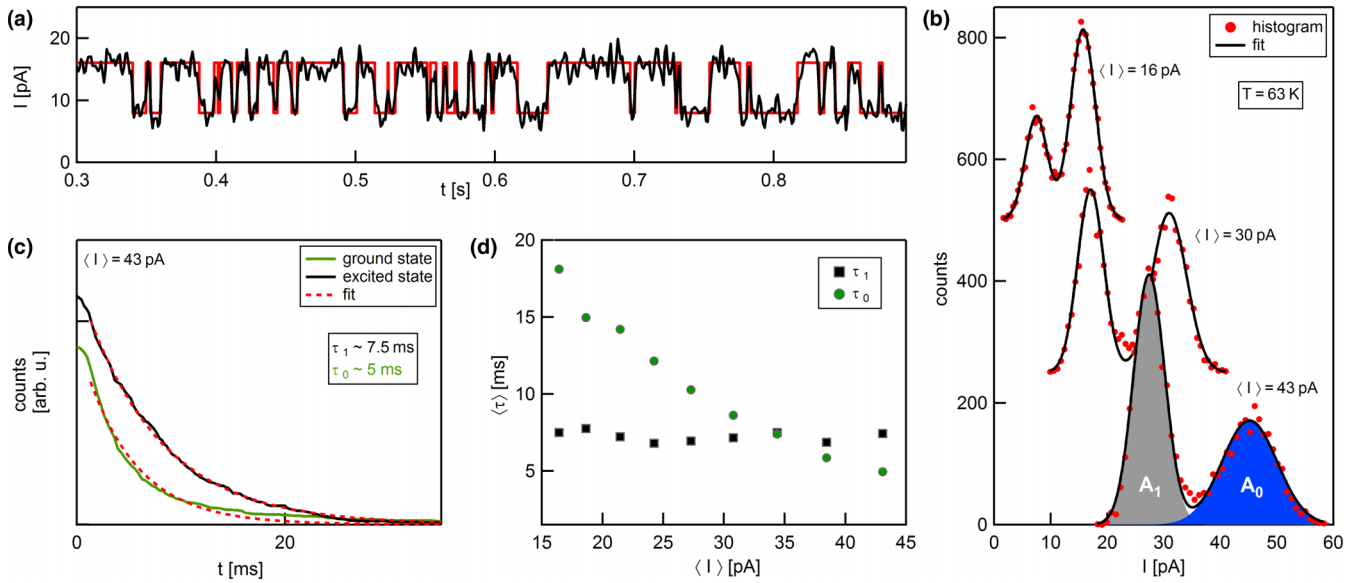

FIG. 2 (color online). (a) Time dependence of the tunneling current (black) at a fixed tip position above a bright protrusion of the 1×3 structure at 63 K. Two distinct levels are evident, corresponding to the 1×3 and 1×2 phases of Si(553)-Au. The red curve represents the result of a threshold analysis. (b) Histograms of the transient tunneling current for different average currents $\langle I \rangle$. The lifetimes $\langle \tau_0 \rangle / \langle \tau_1 \rangle$ are determined from cumulative histograms of the residence times for the ground and excited state as illustrated for $\langle I \rangle = 43$ pA in (c) and plotted versus the average current $\langle I \rangle$ in (d). At $\langle I \rangle \approx 35$ pA the lifetime of the ground state ($\langle \tau_0 \rangle$, green) falls below that of the excited state ($\langle \tau_1 \rangle$, black). While $\langle \tau_0 \rangle$ decreases with $\langle I \rangle$, $\langle \tau_1 \rangle$ remains constant, reflecting the spontaneous decay of the excited 1×2 state into the 1×3 ground state.

tunneling current whereas $\langle \tau_1 \rangle$ remains essentially constant. Hence the excited state has a constant lifetime, irrespective of the tunneling current, and thus shows monostable behavior. This implies that there is no energy barrier for the decay of the excited state into the ground state. This is quite different compared to other surface phases, analyzed in Refs. [7,9,40], for which the STM-induced metastable states exhibited finite barriers to decay.

Doping is known to play a crucial role in determining the detailed structure of atomic chains [41]. This fact motivates the following scenario to explain our experimental observations. Electrons tunnel from the tip into the sample and have a finite probability to temporarily dope the surface electronic system. This doping destabilizes the original 1×3 ground state, which reorganizes into a 1×2 phase [42]. The injected charge has a finite residence time and is eventually drained into the bulk. As a result the system relaxes to its ground state, where it remains until the next doping process.

This scenario is consistent with all our experimental observations. The decrease of the time constant $\langle \tau_0 \rangle$ with current results from the increased frequency of excitation, while $\langle \tau_1 \rangle$ depends only on the decay mechanism and thus is independent of the current [43]. Despite the very different excitation mechanism, this aspect of Si(553)-Au is reminiscent of optical excitation in molecular excimer systems, for which the excitation rate is dependent on light intensity while the decay rate is not. This difference results in a saturation of the excited state occupancy at high intensity. The excited state also bears a resemblance to a polaron, where the structure relaxes as a consequence of the presence of a charge.

In our scenario the fluctuations arise from fast switching between the 1×3 and 1×2 phases. Consequently, significant fluctuations of the tunneling current at constant tip height are only expected on locations in the Si(553)-Au structure where the difference in apparent height between 1×2 and 1×3 is large, i.e., atop the bright protrusions of the 1×3 phase. The most pronounced fluctuations are indeed detected at these sites (see the Supplemental Material [36]).

For charge injection, the excitation rate should depend primarily on the current, and exhibit only a weak temperature dependence. For the charge decay, however, different temperature-dependent mechanisms may exist. Phonon scattering may assist the coupling of excess charge in the surface states with the bulk band structure. Another mechanism is the bulk conductivity: an isolated excess charge may only decay if the surrounding bulk material has finite conductivity, which is a strong function of temperature due to the freeze-out of charge carriers in the semiconducting substrate at low temperatures [16,17]. In that case the transition current is expected to depend on the doping concentration. Although determining the dominant mechanism of charge decay on Si(553)-Au is beyond the scope of this work, in both cases (phonon scattering and freeze-out of charge carriers) a strong increase of the lifetime $\langle \tau_1 \rangle$ is expected for lower temperatures [44]. This results in both

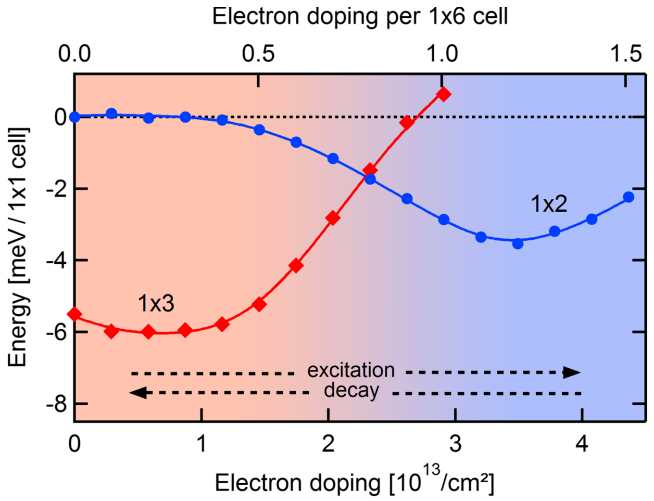

FIG. 3 (color online). Relative total energy of the 1×3 (red) and 1×2 (blue) phase as a function of electron doping. Above a doping level of $\sim 2 \times 10^{13}$ cm^{-2} the 1×2 phase becomes energetically preferred. The arrows indicate the changes of the doping level that cause switching between the two phases.

lower fluctuation rates and a lower transition current, as observed in the experiment (compare Fig. 1).

Our scenario of a charge-induced phase transition is also supported by DFT investigations of the behavior of Si(553)-Au in the presence of excess charge. Figure 3 shows the change in surface energy of the 1×3 and 1×2 phases reported in Ref. [25], as a function of excess electronic charge added to the neutral surface [45]. At zero and low doping concentrations the 1×3 phase is most stable, as previously shown [25]. With increasing electron doping the 1×3 phase becomes progressively less favorable while the 1×2 phase becomes more stable. Above an excess electron concentration of $\sim 2 \times 10^{13}$ cm^{-2} the 1×2 phase is energetically preferred [46]. Upon further increasing the doping, the 1×3 phase becomes unstable and spontaneously collapses to 1×2. This crossover is consistent with our proposed explanation that the observed phase transition is induced by electron doping.

It is interesting to compare our results to STM-induced phase transitions in other systems. The phase transition in Si(553)-Au is dynamic and monostable, with an unusual temperature dependence resulting in higher excitation probabilities at lower temperatures. A similar dependence on current and temperature has been observed on Sn/Ge(111) [11]. Contrasting with our observations where the current-induced 1×2 phase does not appear elsewhere in the phase diagram, the low temperature phase on Sn/Ge(111) exhibits the same $\sqrt{3} \times \sqrt{3}$ appearance as the room temperature phase which is known to be a fluctuating 3×3 phase [47–49]. Furthermore, the fluctuation rate on Sn/Ge(111) remains almost constant below 20 K [53]. For Si(553)-Au the fluctuation rate approaches zero for both high and low temperatures because the system is always driven to one of the two phases. These differences suggest that the phase transitions in Si(553)-Au and Sn/Ge(111) are governed by fundamentally different mechanisms. Despite these differences, the similar current and temperature dependence of the surface symmetry as on Sn/Ge(111) and our identification of a novel mechanism underlying the current induced surface instability may shed light on related nonequilibrium effects observed on, e.g., Sn/Ge(111) or Si(100) surfaces.

In summary, current-induced random telegraph switching is observed between two phases of chains on Si(553)-Au. Analysis of the statistical characteristics of this switching gives the lifetimes of the two phases. An analogy is found to photon-induced structural transitions such as excimers, where the dynamics is not dominated by conformational energy barriers but by the lifetime of the electronically excited state. Together with density-functional theory a scenario is proposed in which electrons injected by the STM tip cause transient doping of the atomic chains, temporarily stabilizing a nominally higher-energy phase for doping levels above a threshold value. Such transient doping by electron injection from a STM tip provides access to hidden 1D phases that cannot be investigated by conventional atom doping. Extra dopant atoms interrupt an atom chain, thereby causing a strong perturbation of the surrounding chain sections [32,54]. The doping method practiced here is less disruptive and allows continuous doping. It may be viewed as analog to the static electron transfer by indirect doping of two-dimensional cuprates, ruthenates, and other complex oxides. Those have produced many exciting results [55], which may be transferable to 1D using transient doping.

Funding by the federal state Mecklenburg-Vorpommern within the project Nano4Hydrogen is gratefully acknowledged (S. P., I. B., K. H. M.-B.). P. C. S. acknowledges support by the U.S. DOE Office of Basic Energy Sciences, Materials Sciences and Engineering Division, through the Oak Ridge National Laboratory. This work was supported by the Office of Naval Research through the Naval Research Laboratory's Basic Research Program (SCE). Computations were performed at the DOD Major Shared Resource Centers at AFRL and ERDC. I. B. acknowledges fruitful discussions with V. v. Oeynhausen and J. Tiggesbäumker.

*ingo.barke@uni-rostock.de

[1] H. Ichikawa *et al.*, Nat. Mater. **10**, 101 (2011).
[2] J. B. Birks, Rep. Prog. Phys. **38**, 903 (1975).
[3] H. Kandori, Y. Shichida, and T. Yoshizawa, Biochemistry (Moscow) **66**, 1197 (2001).
[4] T. Fennel, K.-H. Meiwes-Broer, J. Tiggesbäumker, P.-G. Reinhard, P. M. Dinh, and E. Suraud, Rev. Mod. Phys. **82**, 1793 (2010).
[5] C. Bostedt *et al.*, Phys. Rev. Lett. **108**, 093401 (2012).
[6] A. Cavalleri, Cs. Tóth, C. W. Siders, J. A. Squier, F. Ráksi, P. Forget, and J. C. Kieffer, Phys. Rev. Lett. **87**, 237401 (2001).

[7] P. Tegeder, J. Phys. Condens. Matter **24**, 394001 (2012).
[8] J. A. Stroscio and D. M. Eigler, Science **254**, 1319 (1991).
[9] S. Yoshida, T. Kimura, O. Takeuchi, K. Hata, H. Oigawa, T. Nagamura, H. Sakama, and H. Shigekawa, Phys. Rev. B **70**, 235411 (2004).
[10] K. Sagisaka, D. Fujita, and G. Kido, Phys. Rev. Lett. **91**, 146103 (2003).
[11] S. Colonna, F. Ronci, A. Cricenti, and G. Le Lay, Phys. Rev. Lett. **101**, 186102 (2008).
[12] A. van Houselt and H. J. W. Zandvliet, Rev. Mod. Phys. **82**, 1593 (2010).
[13] J. Schaffert, M. C. Cottin, A. Sonntag, H. Karacuban, C. A. Bobisch, N. Lorente, J.-P. Gauyacq, and R. Möller, Nat. Mater. **12**, 223 (2013).
[14] K. Seino, W. G. Schmidt, and F. Bechstedt, Phys. Rev. Lett. **93**, 036101 (2004).
[15] J. M. Soler, A. Baro, N. García, and H. Rohrer, Phys. Rev. Lett. **57**, 444 (1986).
[16] M. Ono, A. Kamoshida, N. Matsuura, E. Ishikawa, T. Eguchi, and Y. Hasegawa, Phys. Rev. B **67**, 201306 (2003).
[17] I. Brihuega, O. Custance, M. M. Ugeda, N. Oyabu, S. Morita, and J. M. Gómez-Rodríguez, Phys. Rev. Lett. **95**, 206102 (2005).
[18] K. Sagisaka and D. Fujita, Phys. Rev. B **71**, 245319 (2005).
[19] T. Mitsui and K. Takayanagi, Phys. Rev. B **62**, R16251 (2000).
[20] M. Lastapis, M. Martin, D. Riedel, L. Hellner, G. Comtet, and G. Dujardin, Science **308**, 1000 (2005).
[21] V. Iancu and S.-W. Hla, Proc. Natl. Acad. Sci. U.S.A. **103**, 13718 (2006).
[22] J. Crain and D. Pierce, Science **307**, 703 (2005).
[23] J. N. Crain, J. L. McChesney, F. Zheng, M. C. Gallagher, P. C. Snijders, M. Bissen, C. Gundelach, S. C. Erwin, and F. J. Himpsel, Phys. Rev. B **69**, 125401 (2004).
[24] I. Barke, F. Zheng, T. K. Rügheimer, and F. J. Himpsel, Phys. Rev. Lett. **97**, 226405 (2006).
[25] S. C. Erwin and F. J. Himpsel, Nat. Commun. **1**, 58 (2010).
[26] P. C. Snijders, S. Rogge, and H. H. Weitering, Phys. Rev. Lett. **96**, 076801 (2006).
[27] P. C. Snijders, P. S. Johnson, N. P. Guisinger, S. C. Erwin, and F. J. Himpsel, New J. Phys. **14**, 103004 (2012).
[28] J. R. Ahn, P. G. Kang, K. D. Ryang, and H. W. Yeom, Phys. Rev. Lett. **95**, 196402 (2005).
[29] J. S. Shin, K.-D. Ryang, and H. W. Yeom, Phys. Rev. B **85**, 073401 (2012).
[30] P. C. Snijders and H. H. Weitering, Rev. Mod. Phys. **82**, 307 (2010).
[31] S. C. Erwin and P. C. Snijders, Phys. Rev. B **87**, 235316 (2013).
[32] I. Barke, S. Polei, V. v. Oeynhausen, and K.-H. Meiwes-Broer, Phys. Rev. Lett. **109**, 066801 (2012).
[33] I. Barke, F. Zheng, S. Bockenhauer, K. Sell, V. v. Oeynhausen, K. H. Meiwes-Broer, S. C. Erwin, and F. J. Himpsel, Phys. Rev. B **79**, 155301 (2009).
[34] G. Kresse and J. Hafner, Phys. Rev. B **47**, 558 (1993).
[35] G. Kresse and J. Furthmüller, Phys. Rev. B **54**, 11169 (1996).
[36] See Supplemental Material at http://link.aps.org/supplemental/10.1103/PhysRevLett.111.156801 for a movie.
[37] S. Polei *et al.* (to be published).
[38] The apparent 1×6 periodicity observed on the Si-step edge does not reflect the 1×6 antiferromagnetic spin ordering on the step edge proposed in Ref. [25] because it is also observed with a nonmagnetic W tip.
[39] Y. Yuzhelevski, M. Yuzhelevski, and G. Jung, Rev. Sci. Instrum. **71**, 1681 (2000).
[40] Y. Takagi, Y. Yoshimoto, K. Nakatsuji, and F. Komori, Surf. Sci. **559**, 1 (2004).
[41] S. C. Erwin, I. Barke, and F. J. Himpsel, Phys. Rev. B **80**, 155409 (2009).
[42] This reorganization involves only small local displacements of Si step-edge atoms and does not require any bond breaking or atomic diffusion.
[43] We also considered mechanisms based on the electric field between tip and sample. The temperature dependence of the transition (see Fig. 1), its dynamic properties, and the comparison to theory (Fig. 3) render such mechanisms unlikely.
[44] Note though that the injection of electrons and the resulting symmetry changes will excite many phonon modes, which could thus prevent a complete freezing out of phonon scattering mediated decay modes.
[45] The structural details of the honeycomb chain do not significantly affect the convergence of the total energy in the DFT calculations. Hence we were able to analyze the doping dependent total energy of phases with periodicities matching those observed experimentally, even though the precise structural details of the doped 1×2 phase in our experiment remain unknown.
[46] A simple check for plausibility can be made by considering a single injected electron that is homogeneously distributed over one 1×6 unit cell which corresponds to the smallest common cell for both phases. This results in a doping concentration of $\approx 3 \times 10^{13}$ cm^{-2}. This matches the order of magnitude of the relevant doping range as predicted by theory (see the upper axis in Fig. 3).
[47] J. Avila, A. Mascaraque, E. G. Michel, M. C. Asensio, G. Le Lay, J. Ortega, R. Pérez, and F. Flores, Phys. Rev. Lett. **82**, 442 (1999).
[48] T. Shirasawa, H. Tochihara, K. Kubo, W. Voegeli, and T. Takahashi, Phys. Rev. B **81**, 081409 (2010).
[49] Note that the origin of the low temperature $\sqrt{3} \times \sqrt{3}$ on Sn/Ge(111) is still under debate [11,50–52].
[50] H. Morikawa, S. Jeong, and H. W. Yeom, Phys. Rev. B **78**, 245307 (2008).
[51] H. Morikawa and H. W. Yeom, Phys. Rev. Lett. **102**, 159601 (2009).
[52] S. Colonna, F. Ronci, A. Cricenti, and G. Le Lay, Phys. Rev. Lett. **102**, 159602 (2009).
[53] F. Ronci, S. Colonna, A. Cricenti, and G. Le Lay, J. Phys. Condens. Matter **22**, 264003 (2010).
[54] H. S. Yoon, S. J. Park, J. E. Lee, C. N. Whang, and I.-W. Lyo, Phys. Rev. Lett. **92**, 096801 (2004).
[55] E. Dagotto, Science **309**, 257 (2005).